

Chapter 4

On convergence and aspect ratio

4.1 Convergence criteria

The two convergence criteria for the Grisham algorithm are:

1. the ratio of the compressive stress $(\sigma_{x_c}, \sigma_{y_c})$ divided by the modified critical stress $(\sigma_{x_{cr}}, \sigma_{y_{cr}})$ must approach one $[\frac{\sigma_{x_c}}{\sigma_{x_{cr}}} \rightarrow 1; \frac{\sigma_{y_c}}{\sigma_{y_{cr}}} \rightarrow 1]$, and
2. the difference of the diagonal tension stress $(\sigma_{x_{DT}}, \sigma_{y_{DT}})$ from one iteration to the next must approach zero. $[\sigma_{x_{DT_i}} - \sigma_{x_{DT_{i-1}}} \rightarrow 0; \sigma_{y_{DT_i}} - \sigma_{y_{DT_{i-1}}} \rightarrow 0]$

Figures 4.1 and 4.2 show the convergence data for the example problem considered in Chapters 2 and 3, as a function of the iteration count (the stopping criteria are disabled). It is evident from the graphs that the stresses in the x - and y - directions, for the second convergence criterion, converge within five iterations. This is to within a 0.037 % error (taken relative to the final diagonal tension stress) and well within the 2 % margin allowed. The negative value at iteration three, on the graph for the second convergence criterion, is acceptable since convergence is not expected to be monotonic.

After another two iterations, the first convergence criterion converges to a value of one for both the x - and y - directions. This is because the first convergence criterion depends on the diagonal tension stress values. The first convergence criterion converges to within a 1.53 % error value which is again well within the 2 % margin allowed.

The diagonal tension stresses from the previous iteration are subtracted from the membrane stresses in the linear finite element stress results of the current iteration before they are used in the equations of the Grisham algorithm $(\sigma_{x_i} - \sigma_{x_{DT_{i-1}}}; \sigma_{y_i} - \sigma_{y_{DT_{i-1}}})$. The modified stress values appear in the equation for determining the compressive stress values of the web for each panel, which again are used in the first convergence criterion. Therefore, until the diagonal tension stress values have converged (second convergence requirement), the first convergence criterion will not be satisfied.

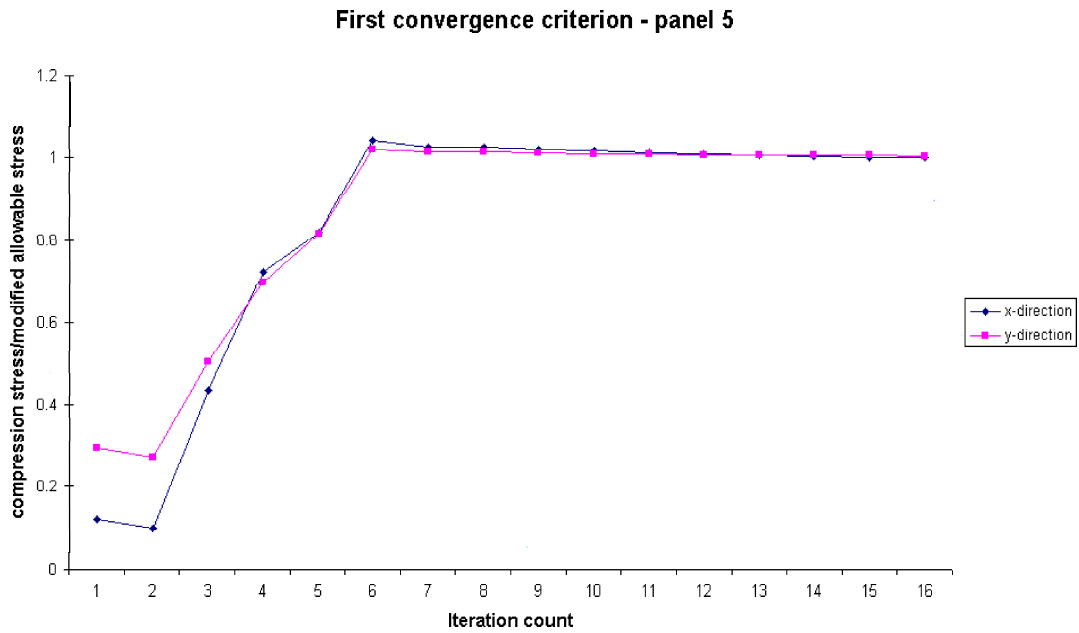


Figure 4.1: First convergence criterion for the Grisham algorithm

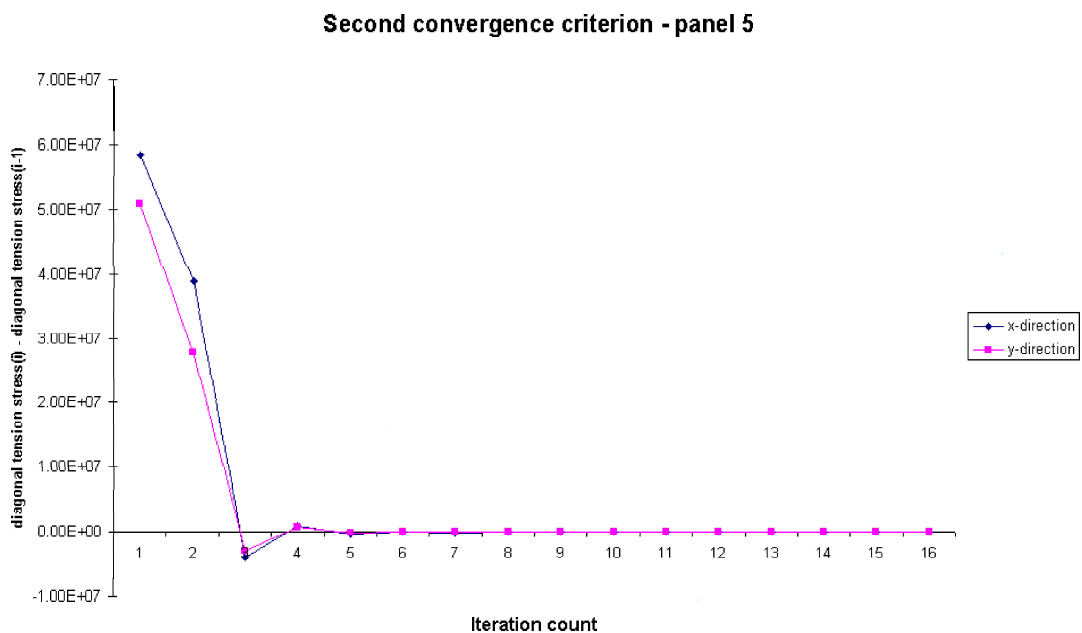


Figure 4.2: Second convergence criterion for the Grisham algorithm

4.2 Effect of β values on convergence

The parameters β_x and β_y are defined by Grisham [6] as the ratios of the buckled stiffness of the web in the x - and y - directions to the unbuckled stiffness of the web in the x - and y - directions respectively ($(\frac{E_{xp}}{E_p})$ and $(\frac{E_{yp}}{E_p})$) for each panel. Since the stiffness of the buckled webs are not known in advance, neither in the x - nor the y - directions initially, these values are estimates of the actual values. In the implementation of the Grisham algorithm, an initial value is assumed for both β_x and β_y for each panel. These values are then varied from iteration to iteration until the first convergence requirement approaches unity. The β values only affect the first convergence requirement (See A.29 and A.30).

When the Grisham algorithm runs through its iteration loop and the first convergence criterion approaches a value larger than unity, the relevant β value is increased and the algorithm re-run. Alternatively, when the first convergence criterion approaches a value smaller than unity, the β value is reduced, after which the analysis is re-run.

In Tables 4.1 to 4.6 the sensitivity of the β values with respect to changes in the web thickness, flange areas and upright areas are summarized. The example considered in Chapters 2 and 3 is again used for this case study. Only panels 2 to 5 are considered since panels 1 and 6 include edge effects. For the flange area investigation, both the upper and lower flanges have the same cross-sectional area.

Both the values of β_x and β_y values drop significantly when the web thickness is increased, showing that they are rather sensitive to web thickness. The β values increase only slightly when the flange and upright areas are increased, showing less sensitivity to the change of flange and upright areas. For all the tests, the values of β_x and β_y remain within $0.565 < \beta_x, \beta_y < 1.098$. These variations can all be accommodated using an *iterative, adaptive correction scheme*.

| Web thickness t | Panel 2 | Panel 3 | Panel 4 | Panel 5 |
|-------------------|---------|---------|---------|---------|
| 0.500 [mm] | 0.978 | 0.972 | 0.995 | 0.978 |
| 0.600 [mm] | 0.960 | 0.958 | 1.018 | 0.962 |
| 0.635 [mm] | 0.952 | 0.950 | 1.076 | 0.952 |
| 0.700 [mm] | 0.937 | 0.935 | 1.098 | 0.941 |
| 0.800 [mm] | 0.892 | 0.894 | 0.770 | 0.912 |
| 0.900 [mm] | 0.854 | 0.850 | 0.822 | 0.872 |
| 1.000 [mm] | 0.785 | 0.790 | 0.794 | 0.828 |

Table 4.1: Variation in β_x as a function of web thickness t

4.3 Effect of aspect ratio on the diagonal tension angle

To investigate the effect of panel aspect ratio on the diagonal tension angle, the aspect ratio of the example from Bruhn is now varied. The results are given in Table 4.7, and reveal a

| Web thickness t | Panel 2 | Panel 3 | Panel 4 | Panel 5 |
|-------------------|---------|---------|---------|---------|
| 0.500 [mm] | 0.966 | 0.972 | 0.966 | 0.958 |
| 0.600 [mm] | 0.922 | 0.940 | 0.938 | 0.922 |
| 0.635 [mm] | 0.898 | 0.928 | 0.930 | 0.912 |
| 0.700 [mm] | 0.845 | 0.891 | 0.905 | 0.885 |
| 0.800 [mm] | 0.714 | 0.818 | 0.852 | 0.824 |
| 0.900 [mm] | 0.664 | 0.732 | 0.790 | 0.772 |
| 1.000 [mm] | 0.565 | 0.641 | 0.696 | 0.688 |

Table 4.2: Variation in β_y as a function of web thickness t

| Flange Area A_f | Panel 2 | Panel 3 | Panel 4 | Panel 5 |
|----------------------------|---------|---------|---------|---------|
| 50.00 [mm ²] | 0.848 | 0.840 | 0.838 | 0.830 |
| 100.00 [mm ²] | 0.910 | 0.910 | 0.898 | 0.890 |
| 200.00 [mm ²] | 0.950 | 0.950 | 0.938 | 0.930 |
| 243.87 [mm ²] | 0.958 | 0.954 | 0.950 | 0.932 |
| 300.00 [mm ²] | 0.966 | 0.964 | 0.952 | 0.938 |
| 435.48 [mm ²] | 0.972 | 0.970 | 0.962 | 0.950 |
| 1000.00 [mm ²] | 0.978 | 0.978 | 0.970 | 0.960 |
| 1500.00 [mm ²] | 0.968 | 0.980 | 0.972 | 0.962 |
| 2000.00 [mm ²] | 0.966 | 0.972 | 0.970 | 0.960 |

Table 4.3: Variation in β_x as a function of flange area A_f

low sensitivity to aspect ratio. This is in agreement with the numerous experimental results generated in the NACA investigation.

| Flange Area A_f | Panel 2 | Panel 3 | Panel 4 | Panel 5 |
|----------------------------|---------|---------|---------|---------|
| 50.00 [mm ²] | 0.902 | 0.894 | 0.894 | 0.896 |
| 100.00 [mm ²] | 0.910 | 0.902 | 0.900 | 0.896 |
| 200.00 [mm ²] | 0.914 | 0.910 | 0.910 | 0.896 |
| 243.87 [mm ²] | 0.918 | 0.912 | 0.910 | 0.896 |
| 300.00 [mm ²] | 0.924 | 0.914 | 0.910 | 0.904 |
| 435.48 [mm ²] | 0.928 | 0.916 | 0.912 | 0.904 |
| 1000.00 [mm ²] | 0.940 | 0.930 | 0.924 | 0.914 |
| 1500.00 [mm ²] | 0.932 | 0.936 | 0.936 | 0.930 |
| 2000.00 [mm ²] | 0.904 | 0.976 | 0.958 | 0.958 |

 Table 4.4: Variation in β_y as a function of flange area A_f

| Upright Area A_u | Panel 2 | Panel 3 | Panel 4 | Panel 5 |
|--------------------------|---------|---------|---------|---------|
| 151.2 [mm ²] | 0.952 | 0.950 | 1.076 | 0.952 |
| 182.9 [mm ²] | 0.951 | 0.949 | 1.078 | 0.953 |
| 217.7 [mm ²] | 0.950 | 0.939 | 1.056 | 0.953 |

 Table 4.5: Variation in β_x as a function of upright area A_u

| Upright Area A_u | Panel 2 | Panel 3 | Panel 4 | Panel 5 |
|--------------------------|---------|---------|---------|---------|
| 151.2 [mm ²] | 0.898 | 0.928 | 0.930 | 0.912 |
| 182.9 [mm ²] | 0.927 | 0.943 | 0.931 | 0.913 |
| 217.7 [mm ²] | 0.939 | 0.947 | 0.934 | 0.925 |

 Table 4.6: Variation in β_y as a function of upright area A_u

| L_y/L_x | α |
|-----------|----------|
| 4.000 | 43.1 |
| 2.330 | 41.2 |
| 1.500 | 39.5 |
| 1.000 | 38.2 |
| 0.667 | 37.1 |
| 0.428 | 36.5 |
| 0.250 | 36.1 |

 Table 4.7: Panel aspect ratio L_y/L_x versus diagonal tension angle α